

EXTRAPOLATING THE EVOLUTION OF GALAXY SIZES TO THE EPOCH OF REIONIZATION

J. STUART B. WYTHE¹, ABRAHAM LOEB²
Draft version September 11, 2021

ABSTRACT

We use data on the high-redshift evolution of the size distribution and luminosity function of galaxies to constrain the relationship between their star formation efficiency and starburst lifetime. Based on the derived scaling relations, we predict the angular sizes and average surface brightnesses of faint galaxies that will be discovered with *JWST*. We find that *JWST* will be able to resolve galaxies at the magnitude limit $m_{\text{AB}} < 31$ out to a redshift of $z \sim 14$. The next generation of large ground-based telescopes will resolve all galaxies discovered with *JWST*, provided they are sufficiently clumpy to enable detection above the bright thermal sky. We combine our constraints with simple models for self regulation of star formation, and show that feedback from supernovae at redshifts $z \gtrsim 3$ is likely mediated through momentum transfer, with the starburst timescale set by the lifetime of the massive stars rather than the dynamical time in the host galactic disk.

Subject headings: galaxies: evolution, formation, high-redshift — cosmology: theory

1. INTRODUCTION

The luminosity function of Lyman-break galaxy candidates discovered at $z \gtrsim 6$ in the Hubble Ultra-Deep Field is described by a Schechter function with a characteristic luminosity that decreases towards higher redshift as expected from the dark matter halo mass-function (e.g. Munoz & Loeb 2010). At low luminosities, the luminosity function is fit as a power-law with a faint end slope of $\alpha \approx -1.8$ that is roughly independent of redshift (McLure et al. 2009; Bouwens et al. 2010; Yan et al. 2010). The shape and overall density of the luminosity function is the primary observable that must be reproduced by any successful model of galaxy formation (e.g. Raičević, Theuns & Lacey 2010, Salvaterra, Ferrara & Dayal 2010; Trenti et al. 2010).

In a recent study, Oesch et al. (2009) have measured the redshift evolution of the scale-length of galactic disks (see also Ferguson et al. 2004; Bouwens et al. 2004). Among a sample of galaxies with constant luminosity, the half-light galaxy radius was found to scale as,

$$R_{\text{gal}} \propto (1+z)^{-m}, \quad (1)$$

with $m = 1.12 \pm 0.17$. This evolution is consistent with the inverse relation between virial radius and redshift [$R_{\text{gal}} \propto (1+z)^{-1}$], that is expected for dark-matter halos assuming a constant halo mass to luminosity ratio (Ferguson et al. 2004; Oesch et al. 2009).

In this *Letter* we model the evolution of galactic disk radii for different parameterised models of self-regulated star formation. We parameterise our models in such a way that the constraints based on the observed size of galaxies are orthogonal to those derived from the slope of the galaxy luminosity function. Based on an empirical determination of parameters of this model, we predict the expected size distribution of galaxies in future surveys with *JWST*, and show that existing observations al-

ready limit the physical processes that govern the global properties of star formation at high redshifts. Where required, we adopt the standard set of cosmological parameters (Komatsu et al. 2009), with density parameters $\Omega_b = 0.044$, $\Omega_m = 0.24$ and $\Omega_\Lambda = 0.76$ for the matter, baryon, and dark energy fractional density, respectively, and $h = 0.72$, for the dimensionless Hubble constant.

2. MODEL

To model high redshift galaxy properties we begin with an expression for the UV luminosity of a galaxy within a dark matter halo of mass M_{halo} ,

$$L \propto f_\star M_{\text{halo}} \frac{\min(t_{\text{SB}}, t_\star)}{t_{\text{SB}} t_\star}, \quad (2)$$

where f_\star is the fraction of baryons turned into stars, t_{SB} is the lifetime of the starburst, and t_\star is the average lifetime of the massive stars ($\gtrsim 8M_\odot$) that affect the feedback through supernova (SN) explosions and dominate the UV luminosity output L . The lifetime of main-sequence stars, $t_{\text{ms}} = 10^{10} \text{yr} (M_{\text{star}}/M_\odot)^{-2.5}$ (Hansen, Kawaler & Steven 1994), implies an average delay time for supernova feedback of $t_\star \sim 7 \times 10^6$ yr for an initial mass function of massive stars $dN/dM_{\text{star}} \propto M_{\text{star}}^{-2.35}$ (Scalo 1986). The value of t_{SB} is thought to be related to the dynamical time (t_{dyn}) of the galactic disk (Kennicutt 1998), which scales as the age of the Universe t_H , namely $t_{\text{dyn}} \sim 3 \times 10^{-3} t_H \approx 3 \times 10^6 \text{yr} [(1+z)/7]^{-3/2}$. Equation (2) implies that the luminosity could become independent of the starburst lifetime at sufficiently high redshifts $z \gtrsim 3$ for which $t_{\text{dyn}} < t_\star$. The mass-to-light ratio is governed by f_\star and t_{SB} , each of which can depend on both M_{halo} and z . We therefore parameterise a general class of models for high redshift galaxy formation using the ratio,

$$f_\star \frac{\min(t_{\text{SB}}, t_\star)}{t_{\text{SB}} t_\star} \propto M_{\text{halo}}^a (1+z)^b. \quad (3)$$

Physically, this quantity is proportional to the inverse of the mass-to-light ratio. This parameterisation can be

swythe@unimelb.edu.au; aloeb@cfa.harvard.edu

¹ School of Physics, University of Melbourne, Parkville, Victoria 3010, Australia

² Astronomy Department, Harvard University, 60 Garden Street, Cambridge, MA 02138, USA

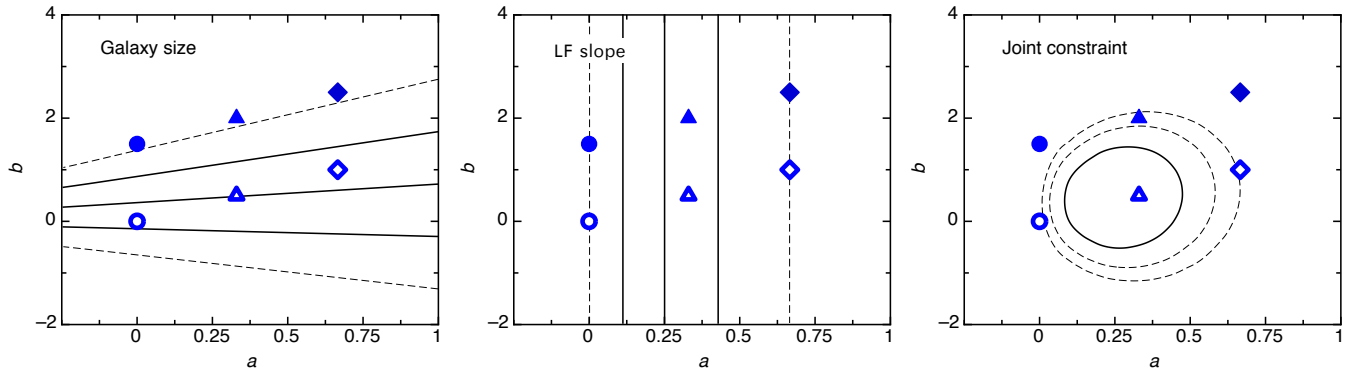


FIG. 1.— *Left Panel:* Contours of parameter combinations (a, b) that give the best fit observed value $m = 1.12$ (central solid line), as well as the ± 1 -sigma (outer solid lines) and ± 2 -sigma combinations (dashed lines). *Central Panel:* Contours of parameter combinations (a, b) that give the best fit observed value $\alpha' = 0.8$ (central solid line), as well as the ± 1 -sigma (outer solid lines) and ± 2 -sigma (dashed lines) combinations. *Right Panel:* The combined constraint from the observables m and α , derived from the product of likelihoods $\mathcal{L}_m = \exp[-(m - 1.12)^2/2(0.17)^2]$ and $\mathcal{L}_\alpha = \exp[-(\alpha' - 0.8)^2/2(0.08)^2]$. The contours represent the 32%, 11% and 4.5% likelihoods, which for a Gaussian distribution contain 68%, 90% and 95.4% of the probability, corresponding to the 1-sigma, 1.5-sigma and 2-sigma ranges for parameter pairs. The model assumes $g = 0$. For comparison, the solid and open circles show the example where there is no feedback, but the starburst timescale is proportional to the dynamical time of the galaxy ($a = 0, b = 3/2$) or the average lifetime of massive stars ($a = 0, b = 0$), respectively. Similarly, the solid and open diamond points show the example of the model in Wyithe & Loeb (2003) that proposes star-formation is limited by the production of the binding energy of the galactic gas in the form of SN-driven winds with $t_{\text{SB}} > t_*$ ($a = 2/3, b = 5/2$) and $t_{\text{SB}} < t_*$ ($a = 2/3, b = 1$). Finally, the solid and open triangle points show the example of a model where star formation is limited by SN-driven winds which deposit momentum rather than energy into the galactic gas, with $t_{\text{SB}} > t_*$ ($a = 1/3, b = 2$) and $t_{\text{SB}} < t_*$ ($a = 1/3, b = 1/2$).

used to describe a range of physical models that predict the unknown variation of the star-formation efficiency and starburst lifetime with redshift and halo mass. Each particular model of the self-regulation of high redshift star formation will yield distinct values for the parameters a and b .

In order to compare the resulting grid of models with the observed evolution in galaxy size we require two further ingredients, namely the virial relation (simplified form valid at high redshift),

$$M_{\text{halo}} \propto R_{\text{vir}}^3 (1+z)^3, \quad (4)$$

and the parameterisation,

$$R_{\text{gal}} \propto R_{\text{vir}} (1+z)^g, \quad (5)$$

to describe the relation between virial radius R_{vir} and the galactic disk scale radius R_{gal} . In the latter expression we expect a parameterisation with $g = 0$ if the disk size³ is set by the adiabatic model of Mo, Mao & White (1998). The above set of relations can be used to find the predicted evolution of the galaxy radius with redshift at a fixed luminosity, yielding

$$m = 1 - g + \frac{1}{3} \frac{b}{a+1}, \quad (6)$$

which can be compared with the observed value of $m = 1.12 \pm 0.17$ (Oesch et al. 2009).

It is also possible to use the observed slope of the luminosity function to constrain the model, thus break-

³ If the gas disk becomes stable to fragmentation at a radius beyond which there is a significant fraction of gas by mass, then the half mass radius of the stellar disk may not equal the scale radius of the gas-disk. However, we find that the disk becomes stable (based on Toomre Q criterion) only at 3-4 scale radii, and therefore that there is a very small fraction of mass at these large radii. Thus, we adopt the assumption $g = 0$ throughout our analysis.

ing the degeneracy between the parameters a and b that arises from application of equation (6). Modelling the galaxy luminosity function using the halo mass function (dn/dM_{halo}) and the simple parameterised model described in equations (2-3) above we find

$$\alpha = \frac{d \log n}{d \log L} = \frac{d \log n}{d \log M_{\text{halo}}} \left| \frac{d \log M_{\text{halo}}}{d \log L} \right| = \frac{1}{a+1} \frac{d \log n}{d \log M_{\text{halo}}}. \quad (7)$$

In the mass range $10^8 M_\odot < M_{\text{halo}} < 10^{10.5} M_\odot$ (near or below the non-linear mass scale at $z \sim 6$), the mass function has the local power-law slope $-2.05 \gtrsim d \log n / d \log M_{\text{halo}} \gtrsim -2.45$. At low luminosities the high redshift galaxy luminosity function is fit as a power-law with faint end slope $\alpha = -1.8$ (McLure et al. 2009; Bouwens et al. 2010; Yan et al. 2010). While the uncertainty in α is large at $z \gtrsim 7$, it is well constrained in the redshift range $4 \lesssim z \lesssim 6$. We estimate a 10% uncertainty in the value of $(d \log n / d \log M_{\text{halo}})$, dominated by the uncertain mass of the host halos. We therefore define $\alpha' \equiv \alpha \times (d \log n / d \log M_{\text{halo}})^{-1}$, and adopt the constraint $\alpha' = 1/(a+1) = 0.8 \pm 0.1$ based on equation (7).

2.1. Parameter constraints

The left hand panel of Figure 1 shows contours of parameter combinations (a, b) that give the best fit observed value $m = 1.12$, as well as the ± 1 -sigma and ± 2 -sigma combinations (equation 6 assuming $g = 0$). The central panel of Figure 1 shows contours of parameter combinations (a, b) that give the best fit observed value $\alpha' = 0.8$, as well as the ± 1 -sigma and ± 2 -sigma combinations (again assuming $g = 0$). The right hand panel shows the combined constraint from both observables, with the contours representing the 32%, 11% and

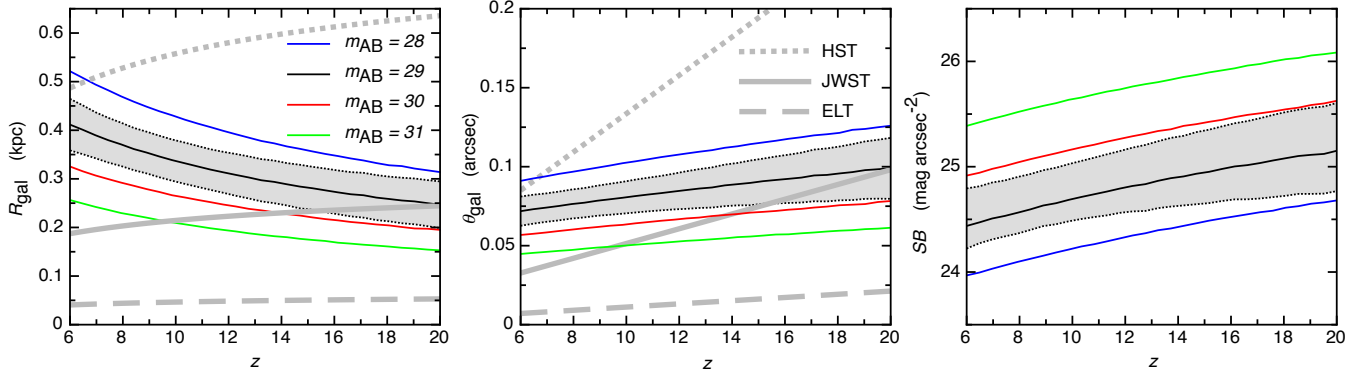


FIG. 2.— The projected relation between galaxy size and redshift, plotted for four values of apparent magnitude. The *Left* and *Central* panels show the physical (R_{gal}) and apparent angular sizes (θ_{gal}) respectively. For comparison (thick grey lines), we also plot the indicative angular resolution $\Delta\theta$ of telescopes with diameters corresponding to *HST* ($D_{\text{tel}} = 2.5$ m), *JWST* ($D_{\text{tel}} = 6.5$ m) and *ELT* ($D_{\text{tel}} = 30$ m). The *Right* panel shows the relation between surface brightness (averaged within the scale radius) as a function of redshift. In each panel, the grey band around the case of $m_{\text{AB}} = 29$ mag shows the 68% range of uncertainty on the mean.

4.5% likelihoods, which for a Gaussian distribution correspond to the 1-sigma, 1.5-sigma and 2-sigma regions for parameters combinations. We find $a = 0.3 \pm 0.15$ and $b = 0.5 \pm 0.6$ (68% range on individual parameters).

3. THE SIZE OF HIGH REDSHIFT GALAXIES

Our empirical constraints can be used to extrapolate galaxy size out to the higher redshifts and lower luminosities that will be observed by the next generation of telescopes. Beginning with equations (2-3) we get,

$$L \propto M_{\text{halo}}^{a+1} (1+z)^b, \quad (8)$$

which when combined with equations (4-5) implies,

$$R_{\text{gal}} \propto L^{\frac{1}{3(1+a)}} (1+z)^{-(1-g+\frac{b}{3(1+a)})} \propto L^{\frac{1}{3(1+a)}} (1+z)^{-m} \\ = R_0 \left(\frac{D_L(z)}{D_L(z_0)} \right)^{\frac{2}{3(1+a)}} 10^{\frac{m_{\text{AB},0} - m_{\text{AB}}}{7.5(a+1)}} \left(\frac{1+z}{1+z_0} \right)^{-m} \quad (9)$$

where D_L is the luminosity distance, m_{AB} is the apparent galaxy magnitude, and $m_{\text{AB},0}$ is the apparent magnitude of galaxies from which the normalization of the relation (R_0) is measured at redshift z_0 . The normalisation of this relation is calibrated using observed galaxy sizes at $z \sim 7-8$ (Oesch et al. 2009). We average the prediction over the three independent points⁴ having $(z_0, R_0, m_{\text{AB},0}) = (7, 0.5 \pm 0.1, 27.8)$, $(7, 0.75 \pm 0.1, 26.6)$, and $(8, 0.4 \pm 0.1, 28.1)$, and over distributions $m = 1.12 \pm 0.17$ and $\alpha = 0.3 \pm 0.15$. The resulting relation is shown in Figure 2 as a function of redshift for four values of apparent magnitude. In the case of $m_{\text{AB}} = 29$ mag, the grey band shows the 68% range of uncertainty on the mean radius. The left and central panels show the physical and apparent angular sizes (θ_{gal}), respectively. Galaxies of fixed apparent magnitude have smaller physical sizes (but larger angular sizes) at higher redshift.

For comparison, we also plot in Figure 2, the indicative angular resolutions of telescopes with diameters corresponding to *HST* ($D_{\text{tel}} = 2.5$ m), *JWST* ($D_{\text{tel}} = 6.5$ m)

and an extremely large telescope (*ELT*; $D_{\text{tel}} = 30$ m)

$$\Delta\theta = \frac{1.22\lambda}{D_{\text{tel}}} \approx 0.085 \left(\frac{1+z}{7} \right) \left(\frac{D_{\text{tel}}}{2.5} \right)^{-1}. \quad (10)$$

Here we have calculated the resolution at the observed wavelength of the redshifted Ly α line $\lambda = 1216(1+z)\text{\AA}$. This simple comparison suggests that galaxies with an apparent magnitude of $m_{\text{AB}} = 28$ mag (1 magnitude fainter than the *HST* WFC3/IR limit) have an angular size of $\theta_{\text{gal}} \sim 0.1''$, which is at the limit of *HST* resolution (Oesch et al. 2009). Fainter galaxies at higher redshifts cannot be resolved by *HST*. The larger aperture of *JWST* will allow the study of galaxy structure at higher redshift and fainter fluxes (Windhorst et al. 2008). For example, galaxies with $m_{\text{AB}} = 29$ mag will be resolved out to at least $z \gtrsim 15$. Moreover, *JWST* will be able to resolve galaxies at the magnitude limits of $m_{\text{AB}} < 30$ and $m_{\text{AB}} < 31$ out to $z \sim 10$ and $z \sim 14$, respectively. Galaxies at yet higher redshifts or fainter fluxes would appear point-like. Bright galaxies are known to become rarer toward high redshift (e.g. Bouwens et al. 2010; Yan et al. 2010), and the discovery of such very high redshift galaxies by *JWST* could be limited by its relatively small field of view (e.g. Munoz & Loeb 2010). However, our extrapolation suggests that an *ELT* would be able to resolve all galaxies detectable with *JWST*.

The above discussion refers only to angular resolution and neglects surface brightness sensitivity. Calculation of the details of surface brightness sensitivity (see, e.g. Windhorst et al. 2008) are beyond the scope of this *Letter*. However, we note that faint, high-redshift galaxies are always below the surface brightness of the sky. Therefore, in order to measure the details of a high redshift galaxy profile, an *HST* observation must achieve a very high signal-to-noise ratio on the zodiacal sky (of order 10^3 per pixel) so that the background would be reliably subtracted (Hathi et al. 2008). The right panel of Figure 2 shows the average surface-brightness within the scale-radius of galaxies of various magnitudes as a function of redshift. Galaxies with $m_{\text{AB}} = 29$ mag show ~ 24.5 magnitudes per square arcsecond at $z \sim 6$, becoming fainter by only a modest amount towards $z \sim 20$. The

⁴ Uncertainty in R_0 is the standard error on the mean.

plotted curves should be compared to the space based value for the zodiacal sky in the K-band of ~ 22.5 magnitudes per square arcsecond (Windhorst et al. 2010), or the ground based K-band value of ~ 14 magnitudes per square arcsecond for the thermal sky. The difference in sky brightness between the ground and space implies that *HST* is equivalent in sensitivity (but not in resolution) to a 150 m ground-based telescope for the purpose of imaging resolved high redshift galaxies. Thus, a ground-based *ELT* will not be competitive with *HST* or *JWST*, since it must overcome the much brighter sky. As a result, even though all high redshift galaxies discovered with *JWST* could be resolved by an *ELT*, their surface brightness will render their extended structure undetectable. However, high redshift galaxies are observed to be very clumpy owing to the presence of star forming regions (Hathi et al. 2008), and an *ELT* will be more sensitive to these unresolved clumps than to diffuse structure, owing to the higher resolution in addition to larger collecting area. Indeed, *HST* is comparable to *only* a 20 m ground based telescope with respect to point source sensitivity (but without the resolution of a 20 m aperture). Thus, if high redshift galaxies are sufficiently clumpy, then an *ELT* may be able to obtain close to the theoretical resolution shown in the central panel of Figure 2.

4. STAR FORMATION MODEL CONSTRAINTS

A range of simple models for the process governing star formation can be compared to the constraints on parameters a and b . We consider three simple models for the possible feedback. The first is a model where there is no self regulation of star formation. The second and third models describe the evolution in cases where the star formation is limited by SN feedback, and the interaction between the SN driven wind and the galactic gas conserves energy and momentum, respectively. In each of these three cases we consider scenarios where the lifetime of the starburst is proportional to the galaxy dynamical time and to the lifetime of massive stars, respectively. Altogether, we have 6 model predictions for m and α' with which to compare our constraints.

4.1. Models without feedback

We begin with feedback-free models in which the star formation efficiency $f_\star \propto M_\star/M_{\text{halo}} = \text{const.}$ We first consider the case where the natural timescale for the starburst is proportional to the galaxy dynamical time, $t_{\text{SB}} \propto t_{\text{dyn}} \propto (1+z)^{-3/2}$, which implies

$$f_\star \frac{\min(t_{\text{SB}}, t_\star)}{t_{\text{SB}} t_\star} \propto \frac{f_\star}{t_{\text{dyn}}} \propto \frac{M_{\text{halo}}^0 (1+z)^0}{(1+z)^{-3/2}} \propto M_{\text{halo}}^0 (1+z)^{3/2}, \quad (11)$$

yielding $a = 0$ and $b = 3/2$. This parameter combination is shown by the solid circles in Figure 1 for comparison with the present constraints. We find that this simple model is inconsistent with both the observed evolution in R_{gal} and the observed luminosity function slope at the 2-sigma level. The combined constraint rules out this model at high confidence.

However, at the high redshifts when the dynamical time is shorter than the average lifetime of massive stars, the same luminosity may be achieved with a lower star

formation rate than in the model described above,

$$f_\star \frac{\min(t_{\text{SB}}, t_\star)}{t_{\text{SB}} t_\star} \propto \frac{f_\star}{t_\star} \propto M_{\text{halo}}^0 (1+z)^0, \quad (12)$$

yielding $a = b = 0$ for galaxies in this case. Such a model (shown by the open circular symbols) is ruled out by the slope of the luminosity function at the 2-sigma level, but is consistent with the observed evolution in galaxy radius. The combined constraint rules out this model at high confidence.

4.2. Models with feedback through energy conservation

We next consider models including self-regulation of star formation by supernovae feedback. The model of Wyithe & Loeb (2003) assumes that star formation is limited by the transfer of energy from SN-driven winds when it is equal to the binding energy to the galactic gas (Dekel & Woo 2002). The model asserts that stars form with an efficiency f_\star out of the gas that collapses and cools within a dark matter halo and that a fraction F_{SN} of each supernova energy output, E_{SN} , heats the galactic gas mechanically. The mechanical feedback will halt the star formation once the cumulative energy returned to the gas by supernovae equals its binding energy (assuming negligible radiative losses for a sufficiently rapid starburst). Hence, in this model the limiting stellar mass is set by the condition

$$\frac{M_\star}{w_{\text{SN}}} E_{\text{SN}} F_{\text{SN}} = E_{\text{b}} = \frac{1}{2} \frac{\Omega_{\text{b}}}{\Omega_{\text{m}}} M_{\text{halo}} v_{\text{c}}^2, \quad (13)$$

where w_{SN} is the mass in stars (in M_\odot) per supernova explosion. Equations (4) and (13) imply that the total mass in stars, $M_\star = (f_\star \Omega_{\text{b}} / \Omega_{\text{m}}) M_{\text{halo}}$, scales as

$$M_\star \propto M_{\text{halo}}^{5/3} (1+z), \quad (14)$$

and hence the star formation efficiency scales as $f_\star \propto M_{\text{halo}}^{2/3} (1+z)$. Thus, smaller galaxies are less efficient at forming stars, but a galaxy of fixed mass is more efficient at forming stars at higher redshift.

In a model where the starburst lifetime is proportional to the galaxy dynamical time, we find

$$\frac{f_\star}{t_{\text{dyn}}} \propto \frac{M_{\text{halo}}^{2/3} (1+z)}{(1+z)^{-3/2}} \propto M_{\text{halo}}^{2/3} (1+z)^{5/2}. \quad (15)$$

This model can therefore be parameterised in terms of the combination $a = 2/3$, and $b = 5/2$ for galaxies, which is shown by the solid diamonds in Figure 1. This simple supernovae driven feedback model is inconsistent with the observed evolution in R_{gal} and the luminosity function slope at the 2-sigma level. The combined constraint rules out this model at high confidence.

However, at high redshifts $z \gtrsim 3$ when the disk dynamical time is shorter than the lifetime of a massive star $t_\star \sim 10^7 \text{yr}$, we note that SN feedback will be less efficient, and the star formation efficiency could exceed the self regulated value of f_\star described above. In particular,

$$\frac{f_\star}{t_\star} \propto \frac{M_{\text{halo}}^{2/3} (1+z)}{t_\star} \propto M_{\text{halo}}^{2/3} (1+z), \quad (16)$$

yielding $a = 2/3$, and $b = 1$ for galaxies in this case (open diamond symbols). Such a model is consistent with the

observed evolution of galaxy size, but inconsistent with the slope of the luminosity function at the 2-sigma level.

4.3. Models with feedback through momentum conservation

Finally, we consider a model where the SN-driven winds conserve momentum in their interaction with the galactic gas rather than energy. In this case the limiting stellar mass is set by the condition

$$\frac{M_{\star}}{v_{\text{SN}}} \frac{E_{\text{SN}}}{c} F_{\text{SN}} = \frac{1}{2} \frac{\Omega_{\text{b}}}{\Omega_{\text{m}}} M_{\text{halo}} v_{\text{c}}. \quad (17)$$

In a model where the starburst timescale is proportional to the galaxy dynamical time, we find

$$\frac{f_{\star}}{t_{\text{dyn}}} \propto M_{\text{halo}}^{1/3} (1+z)^2. \quad (18)$$

This model (solid triangles), represented by $a = 1/3$ and $b = 2$, is consistent with the constraints from α , but ruled out at the 2-sigma level by the constraints from the evolution of galaxy radius. If instead the lifetime of massive stars sets the starburst timescale, we find

$$\frac{f_{\star}}{t_{\star}} \propto M_{\text{halo}}^{1/3} (1+z)^{1/2}, \quad (19)$$

which is represented by $a = 1/3$ and $b = 1/2$, and is plotted as the open triangles in Figure 1. This model is consistent with both the constraints from m and α' .

Our results imply that SN feedback in high redshift galaxies occurs through the transfer of momentum between the SN-driven wind and the galactic gas, and that

the starburst timescale is set by the average lifetime of massive stars rather than the dynamical time of the host galactic disk.

5. DISCUSSION

We have used the observed redshift evolution of disk sizes, and luminosity function of galaxies to constrain the relationship between star formation efficiency and starburst lifetime. We find that supernova feedback in high redshift galaxies is likely mediated through momentum transfer with the starburst timescale dictated by the average lifetime of the massive stars, t_{\star} . The latter result follows naturally from the fact that the dynamical time of galactic disks becomes shorter than $t_{\star} \sim 10^7$ yr at redshifts $z \gtrsim 6$.

We extrapolated the derived scaling relations to predict the angular sizes of galaxies at higher redshifts and fainter fluxes than currently observed. We have found that *JWST* will be able to resolve galaxies with $m_{\text{AB}} < 30$ and $m_{\text{AB}} < 31$ only out to redshifts of $z \sim 10$ and $z \sim 14$, respectively. However, if high redshift galaxies are sufficiently clumpy, so that unresolved star forming regions can be detected above the bright thermal sky, then the next generation of ground-based extremely large telescopes will be able to resolve structure in all galaxies at all redshifts detectable by *JWST*.

We thank Rogier Windhorst for helpful discussions. JSBW acknowledges the support of the Australian Research Council. AL was supported in part by NSF grant AST-0907890 and NASA grants NNX08AL43G and NNA09DB30A.

REFERENCES

- Bouwens, R. J., et al. 2010, arXiv:1006.4360
 Bouwens, R. J., Illingworth, G. D., Blakeslee, J. P., Broadhurst, T. J., & Franx, M. 2004, ApJ, 611, L1
 Dekel, A., & Woo, J. 2003, MNRAS, 344, 1131
 Ferguson, H. C., et al. 2004, ApJ, 600, L107
 Hansen, Carl J.; Kawaler, Steven D. (1994). Stellar Interiors: Physical Principles, Structure, and Evolution. Birkhuser. p. 28. ISBN 038794138X.
 Hathi, N. P., Jansen, R. A., Windhorst, R. A., Cohen, S. H., Keel, W. C., Corbin, M. R., & Ryan, R. E., Jr. 2008, AJ, 135, 156
 Kennicutt, R. C., Jr. 1998, ApJ, 498, 541
 Komatsu, E., et al. 2009, ApJS, 180, 330
 McLure, R. J., Cirasuolo, M., Dunlop, J. S., Foucaud, S., & Almaini, O. 2009, MNRAS, 395, 2196
 Mo, H. J., Mao, S., & White, S. D. M. 1998, MNRAS, 295, 319
 Muñoz, J. A., & Loeb, A. 2010, arXiv:1010.2260
 Oesch, P. A., et al. 2010, ApJ, 709, L21
 Raičević, M., Theuns, T., & Lacey, C. 2010, arXiv:1008.1785
 Salvaterra, R., Ferrara, A., & Dayal, P. 2010, arXiv:1003.3873
 Scalo, J. M. 1986, Fund. Cosmic Phys., 11, 1
 Trenti, M., Stiavelli, M., Bouwens, R. J., Oesch, P., Shull, J. M., Illingworth, G. D., Bradley, L. D., & Carollo, C. M. 2010, ApJ, 714, L202
 Windhorst, R. A., Hathi, N. P., Cohen, S. H., Jansen, R. A., Kawata, D., Driver, S. P., & Gibson, B. 2008, Advances in Space Research, 41, 1965
 Windhorst, R. A., et al. 2010, arXiv:1005.2776
 Wyithe, J. S. B., & Loeb, A. 2003, ApJ, 595, 614
 Yan, H.-J., Windhorst, R. A., Hathi, N. P., Cohen, S. H., Ryan, R. E., O'Connell, R. W., & McCarthy, P. J. 2010, Research in Astronomy and Astrophysics, 10, 867